THE JOURNAL OF BIOLOGICAL CHEMISTRY VOL. 286, NO. 3, pp. 1895–1902, January 21, 2011

Salmonella enterica Response Regulator SsrB Relieves H-NS Silencing by Displacing H-NS Bound in Polymerization Mode and Directly Activates Transcription*[S]

Received for publication, July 15, 2010, and in revised form, November 4, 2010 Published, JBC Papers in Press, November 8, 2010, DOI 10.1074/jbc.M110.164962

Don Walthers[‡], You Li[§¶], Yingjie Liu[§¶], Ganesh Anand[‖], Jie Yan[§¶], and Linda J. Kenney[‡¶1]

From the [‡]Department of Microbiology and Immunology, University of Illinois, Chicago, Illinois 60612 and the [§]Department of Physics, Mechanobiology Institute, and [‖]Department of Biology, [¶]National University of Singapore, Singapore 119007

The response regulator SsrB activates expression of genes encoded within and outside of a pathogenicity island (SPI-2), which is required for systemic infection of *Salmonella*. SsrB binds upstream of the *sifA, sifB,* and *sseJ* effector genes and directly regulates transcription. SsrB also relieves gene silencing by the nucleoid protein H-NS. Single molecule experiments with magnetic tweezers demonstrated that SsrB displaces H-NS from DNA only when it is bound in a polymerization (stiffening) mode and not when H-NS is bound to DNA in the bridging mode. Thus, in contrast to previous views, the polymerization binding mode of H-NS is the relevant form for counter-silencing by SsrB. Our results reveal that response regulators can directly activate transcription and also relieve H-NS silencing. This study adds to the repertoire of mechanisms by which NarL/FixJ subfamily members regulate transcription. Because SsrB-dependent promoters are diversely organized, additional mechanisms of transcriptional activation at other loci are likely.

Salmonella enterica uses multiple type III secretion systems as virulence determinants to modulate host cell processes such as signaling, membrane trafficking, and cytoskeleton dynamics to promote virulence. These protein secretion machines are encoded within horizontally acquired, AT-rich pathogenicity islands. The effectors secreted by the type III secretion systems of *Salmonella* pathogenicity island 1 (SPI-1) promote uptake into nonphagocytic cells. After transiting the epithelium, *Salmonella* encounters host phagocytes and resides in an intracellular vacuole (the *Salmonella*-containing vacuole (SCV)).[2] Effector proteins secreted by SPI-2 are required for the growth and maintenance of this intracellular compartment. The SCV avoids normal endolysosomal trafficking, protects the bacteria from cytotoxic components present in the macrophage cytoplasm, and provides a replication niche. Two hallmarks of SCVs harboring *Salmonella* are a perinuclear localization near the Golgi network and extension from the SCV membrane of *Salmonella*-induced filaments along microtubules toward the cell periphery (1–5). This endosomal tubulation (6) has been extensively studied in epithelial cells, but it is in the macrophage where survival in the SCV is required to promote systemic infection. Although the role of endosomal tubulation remains unclear, *Salmonella*-induced filaments are coincident with *Salmonella* replication (5), and defects in *Salmonella*-induced filament formation correlate with an unstable SCV (7) and severe attenuation of virulence (1).

In this study, we focus on the regulation of the SPI-2 co-regulated effectors *sifA*, *sifB,* and *sseJ*. SifA localizes to the SCV and Sif-containing membranes and interacts with the host protein SKIP (SifA and kinesin-interacting protein) to uncouple the microtubule motor protein kinesin from the SCV (3). SifA inhibits the interaction between SKIP and the G protein Rab9 (8). The SPI-2 effector SseJ has an acetyltransferase/lipase activity and also localizes to the SCV (9, 10). Mutants of *sseJ* displayed a more moderate virulence defect when compared with *sifA* but showed no observable defect in SCV maintenance or Sif formation (11, 12). Although *sseJ* mutants of *Salmonella* are not defective in inducing Sif formation, transient ectopic co-expression of both SifA and SseJ was required for endosomal tubule formation in the absence of *Salmonella* infection (6). Overexpression of activated G protein RhoA with SseJ directed the formation of endosomal tubules in the absence of SifA (6). Taken together, these studies suggest that SifA, SseJ, and various host cell proteins form a complex to modulate the SCV and Sif membrane dynamics. SifB is 30% identical to SifA and localizes to the SCV and Sif membranes, yet it has not been implicated in virulence (12).

Salmonella and related enteric bacteria have evolved a mechanism to selectively silence AT-rich, horizontally acquired DNA, mediated by the nucleoid protein H-NS (13, 14). Overcoming H-NS silencing of SPI-2 is governed by a complex regulatory hierarchy. The response regulator OmpR, the MarR homologue SlyA, and the nucleoid protein Fis contribute directly to activate the *ssrA-ssrB* SPI-2 regulatory locus, which encodes a two-component regulatory system (15–18). Regulation of SPI-2 by PhoP is controversial, but the PhoP-PhoQ two-component system activates other genes required

* This work was supported, in whole or in part, by National Institutes of Health Grant GM-058746. This work was also supported by Veterans Administration Grant 1IO1BX000372 (to L. J. K.), Singapore Ministry of Education Grants R144000192112 and R144000251112 (to J. Y.), and the Mechanobiology Biology Institute, National University of Singapore.

[S] The on-line version of this article (available at http://www.jbc.org) contains supplemental Table 1 and Figs. 1 and 2.

[1] To whom correspondence should be addressed: Dept. of Microbiology and Immunology, University of Illinois, 835 S. Wolcott Ave. (MC 790), Chicago, IL 60612. Fax: 312-996-6415; E-mail: kenneyl@uic.edu.

[2] The abbreviations used are: SCV, *Salmonella*-containing vacuole; qRT-PCR, quantitative RT-PCR; nt, nucleotide; RNAP, RNA polymerase; αCTD, C-terminal domain of α subunit of RNAP; CRP, catabolite repressor protein; pN, piconewton.

for intracellular survival of *Salmonella* (Refs. 19–21 and for a review see Ref. 22). OmpR is at the top of the regulatory hierarchy and binds upstream of the *ssrA* −35 hexamer (16, 17) and directly stimulates transcription.[3] The sensor kinase SsrA responds to unknown signals to presumably phosphorylate the response regulator SsrB. Environmental signals that stimulate SPI-2 expression include low pH, low osmolality, and cation and phosphate limitation. The isolated C terminus of SsrB ($SsrB_C$) binds to DNA and activates transcription (15). SsrB regulates transcription of multiple operons with diverse architectures within SPI-2 (23) and additional genes located elsewhere on the chromosome (15, 24). SsrB-binding sites are located distally upstream or downstream of transcription start sites, at promoter-proximal positions upstream of, or overlapping, the −35 hexamer, or at sites that overlap the −10 hexamer and/or the transcription start site. This repertoire of diversely organized promoters does not suggest a common mechanism of transcriptional control.

Xenogeneic silencing of AT-rich, horizontally acquired DNA, including SsrB-regulated promoters, is mediated by H-NS. Counter-silencing of H-NS requires one or more transcriptional activators, such as SlyA, RovA, or SsrB (reviewed in Ref. 25). How transcription factors function to counter H-NS silencing requires additional mechanistic understanding of how H-NS binds to DNA. Two modes of H-NS binding to DNA have been described using atomic force microscopy and single molecule experiments (26). One is a bridging mode in which H-NS binds DNA and promotes looping and H-NS protein-protein interactions (28). The other polymerization mode leads to DNA stiffening, elongation, and no folding (27). Investigators speculated that these two binding modes were associated with two H-NS *in vivo* activities, compaction of the nucleoid and repression of gene expression. More recent studies revealed an ionic switch between the two modes of H-NS binding (26) and raised the following question. Which mode of H-NS binding is overcome by SsrB? In this study, we show that SsrB promotes H-NS release from DNA bound in the polymerization mode, whereas H-NS bound to DNA in the bridging mode is inert to SsrB.

Based on previous studies, we predicted that SsrB functions as both a counter-silencer of H-NS and as a direct activator of transcription (23). In this study, we demonstrate that SsrB directly stimulates transcription of *sifA*, *sifB,* and *sseJ* by binding upstream of their respective promoters. H-NS selectively silences transcription *in vitro* of *sifA*, *sifB,* and *sseJ*. $SsrB_C$ is able to overcome H-NS repression of transcription. SsrB-dependent activation of *sifA* transcription does not require the C-terminal domain of the α subunit of RNAP (αCTD), suggesting a CRP-type class II activation mechanism. Thus, SsrB regulates transcription of *sifA, sifB,* and *sseJ* by both direct activation and relief of H-NS repression.

EXPERIMENTAL PROCEDURES

Strains, Proteins, and Plasmids—Oligonucleotides are listed in supplemental Table 1. The $SsrB_C$ expression plasmid pKF44, $SsrB_C$ purification, and *S. enterica* serovar Typhimurium strains were described previously (15, 23). The His_6-tagged H-NS expression vector was constructed as follows. *Salmonella* genomic DNA was amplified with primers DW655 and DW656. The resulting product was TOPO-TA cloned into pCR2.1 as described by the manufacturer (Invitrogen) to create plasmid pDW254, and the EcoRI-PstI *hns* fragment was then subcloned into pMPM-T5Ω to create plasmid pDW160 (29). The DNA sequence of the final product was confirmed. His_6-H-NS expression in *Escherichia coli* DH5α was induced with 0.2% arabinose at an A_{600} of 0.3 for 3 h, and the protein was batch-purified with TALON metal affinity resin (Clontech) as suggested by the manufacturer, except that 500 mM NaCl was used in the wash and elution buffers. Protein concentration was determined with the micro BCA kit as directed by the manufacturer (Pierce), and purity was confirmed to be >90% by SDS-PAGE and Coomassie staining.

DNase I Protection Footprinting and Primer Extension—Footprinting and sequencing templates for *sifB* and *sseJ* are described under "*In Vitro* Transcription." The *sifA* template was constructed by PCR amplification of *Salmonella* genomic DNA with primer pairs DW672 and DW715. The resulting product was TOPO-TA cloned into pCR2.1 to create plasmid (pDW89) and then subcloned into pRLG700 as described below to create pDW191. DNase I footprinting with purified His-$SsrB_C$ and ^{32}P-labeled primers DW715 (*sifA*), DW685 (*sifB*), or DW712 (*sseJ*) was performed as described previously (23) but employed a new buffer system. The binding reactions were performed in 60 mM potassium glutamate, 40 mM HEPES, pH 7.4, 2 mM $MgCl_2$, 0.05% Nonidet P-40 (Sigma), and 1 mM DTT. Sequencing templates for primer extension were constructed by PCR amplification of *Salmonella* genomic DNA with primer pairs DW247 and DW249 (*sifA*), DW245 and DW250 (*sifB*), and DW702 and DW696 (*sseJ*). The resulting products were TOPO-TA cloned into pCR2.1 to create plasmids pDW108 (*sifA*), pDW109 (*sifB*), and pDW886 (*sseJ*). Primer extension was performed using radiolabeled oligonucleotides DW249 (*sifA*), DW721 (*sifB*), and DW696 (*sseJ*) as described previously (23). The start sites were verified with a second gene-specific primer (data not shown).

Quantitative RT-PCR (qRT-PCR)—qRT-PCR and data analysis for acid induction assays were performed as described previously (23) on cells grown in N9 minimal medium (20) to an absorbance of 0.4–0.6. The data were generated using the same RNA preparations as described previously and are thus directly comparable with the reported transcript levels of SPI-2 genes. Primer pairs DW460 and DW461 (*sifA*), DW462 and DW463 (*sifB*), and DW717 and DW718 (*sseJ*) were used to quantify transcript levels. Data were normalized to 16 S RNA levels. qRT-PCR on RNA from the *hns* mutants was also performed as described previously (23). As *Salmonella hns* mutants do not grow well in N9 minimal medium, PCN minimal medium was used as a substitute.

In Vitro Transcription—The *sifA, sifB,* and *sseJ* promoters were cloned into pRLG770 (30) as follows. Primer pairs DW671 and DW672 (*sifA*), DW685 and DW686 (*sifB*), and DW712 and DW713 (*sseJ*) were used to amplify *Salmonella*

[3] D. Walthers and L. J. Kenney, unpublished data.

genomic DNA. The resulting products were TOPO-TA-cloned to create plasmids pDW185, pDW699, and pDW888, respectively. The plasmids were digested with EcoRI and HindIII, and the promoter fragments were subcloned into pRLG770 to create plasmids pDW163 (*sifA*) and pDW700 (*sifB*) and pDW890 (*sseJ*). Supercoiled plasmid DNA was purified from *E. coli* DH5α with the Qiagen mini-prep kit. To remove RNases, eluted DNA was suspended in 500 μl of TE, phenol-extracted twice, and ethanol-precipitated. DNA pellets were washed with ethanol multiple times to remove residual phenol (30). Multiple round transcription assays were performed as described (31) with 50 ng of template, 7.5 nM RNAP (Epicenter; 5 nM for *sifB* template), and 2.5 μCi of [γ-^{32}P]UTP (3000 Ci/mmol 10 mCi/ml; PerkinElmer Life Sciences) in the same buffer used for DNase I footprinting but excluding DTT. Prior to addition of RNAP, the indicated concentrations of $SsrB_C$ or H-NS were incubated for 10 min at 37 °C; reactions containing both $SsrB_C$ and H-NS were incubated for an additional 10 min after addition of the second protein. Experiments were repeated three to five times, and representative experiments are depicted in Fig. 3. Transcript sizes were verified by resolving reactions next to products generated with pRLG589 template (data not shown), which contains the *rrnB* P1 promoter encoding an ~190-nt transcript that serves as a molecular weight marker (30). Promoter-specific transcript levels were normalized to the level of RNA-1 in each lane with background subtraction using ImageQuant 5.1 software (GE Healthcare). Fold-activation is relative to the reaction lacking both $SsrB_C$ and H-NS; counter-silencing is relative to the reaction containing 200 nM H-NS but lacking $SsrB_C$. The wild type and αCTD truncation of His_6-β' RNAP used in Fig. 3*D* at a concentration of 20 nM were a kind gift from Wilma Ross and Richard L. Gourse (University of Wisconsin, Madison).

Magnetic Tweezers Experiments—A transverse magnetic tweezers (32) was used to perform the experiments as described previously (26). For Fig. 4, *A* and *B,* the force response of DNA was in the presence of 600 nM H-NS in stiffening buffer (pH 7.4, 50 mM KCl, 24 °C) and in bridging buffer (pH 7.4, 50 mM KCl, 10 mM $MgCl_2$, 24 °C), respectively. At each force, the extension was recorded for 2 min. Data recorded in the last 10 s were used to obtain the final extension and plotted in Fig. 4, all panels. For Fig. 4, *C* and *D,* the force response of DNA was in the presence of 300 nM $SsrB_C$ in stiffening buffer and in bridging buffer, respectively. At each force, the extension was recorded for 2–4 min. For Fig. 4, *E* and *F,* the force response of DNA was in the presence of 300 nM $SsrB_C$ and 600 nM H-NS in stiffening buffer and in bridging buffer, respectively. At each force, the extension was recorded for 2–3 min.

RESULTS

Identification of the sifA, sifB, and sseJ Promoters—A previous study demonstrated that *sifA*, *sifB,* and *sseJ* expression was dependent on *ssrA,* and secretion of the gene products was dependent on the SPI-2 type III secretion systems (33). We used primer extension to identify the location of each promoter and to determine whether transcription from the native chromosomal locus was dependent on the presence of *ssrB*. The results depicted in Fig. 1*A* reveal single, predominant products with *sifA*-specific and *sseJ*-specific primers. The *sifB* primer extension reaction yielded two adjacent robust products and a third product that extended immediately upstream (assigned as +1). This transcript pattern was confirmed with a second primer (data not shown). The *asterisk* in Fig. 1*A* indicates a nonspecific primer extension product that was not observed with the alternate primer (data not shown). A fourth *sifB* product that extended to +10 was also observed. The position of the cluster of *sifB* primer extension products is in agreement with the size of the ~165-nt *sifB in vitro* transcription product (Fig. 3*B*). A similar pattern of multiple proximal transcription start sites was also observed at the *sseA* promoter (23). In the absence of *ssrB* (Fig. 1*A*, indicated by −), primer extension products were not observed, indicating that *ssrB* was required for transcription under these growth conditions.

$SsrB_C$ Binds Upstream of the sifA, sifB, and sseJ Promoters—Primer extension analysis established that transcription of *sifA*, *sifB,* and *sseJ* was dependent on *ssrB*. To determine whether regulation by SsrB was direct, we used DNase I protection footprinting to examine the interaction between SsrB and promoter DNA. Because purified preparations of full-length SsrB were unstable in solution, we employed a C-terminal construct that we previously showed binds to DNA *in vitro* and activates transcription *in vivo* (15, 23). The results are shown in Fig. 1, *B–D*. At *sifA*, increasing concentrations of $SsrB_C$ result in a protection pattern that extends from −84 to −33 with flanking and internal hypersensitive sites (Fig. 1, *B,* marked by *arrows*). In the family member NarL, ~20 bp of DNA was protected by binding (34). Our results are consistent with two, or perhaps three, $SsrB_C$ dimers protecting *sifA* DNA from cleavage. The protection patterns observed with *sifB* and *sseJ* DNA suggest single $SsrB_C$ dimer binding sites between −56 and −32 and between −57 and −33, respectively, both with flanking and/or internal hypersensitive sites. Thus, $SsrB_C$ directly regulates transcription of *sifA*, *sifB,* and *sseJ* by binding upstream of the respective promoters. The presence of hypersensitive sites (23), our experiments with magnetic tweezers (Fig. 4), our recent DNA binding studies with $SsrB_C$ (35), and the requirement for supercoiled templates for *in vitro* transcription (Fig. 3) all indicate that SsrB binding distorts and/or bends the DNA both upstream and downstream of its binding sites.

Transcription of sifA, sifB, and sseJ Requires Both ssrB and Acidic pH—Acid pH is a signal for SPI-2 effector protein secretion, but protein expression has been reported under non-inducing conditions (36–38), including effectors SifA, SifB, and SseJ (39). We used qRT-PCR to quantify the dependence on *ssrB* and to examine acid induction at the native chromosomal *sifA*, *sifB,* and *sseJ* promoters. Wild type or *ssrB* null strains were grown in N9 minimal medium at low (5.8) or high (8.0) pH and harvested in mid-log phase. The results of qRT-PCR using the indicated gene-specific primers are shown in supplemental Fig. 1. Under SPI-2 inducing conditions, pH 5.8, *sifA* showed a strong dependence on *ssrB* (34-fold; supplemental Fig. 1, *panel A*). The acid pH induction

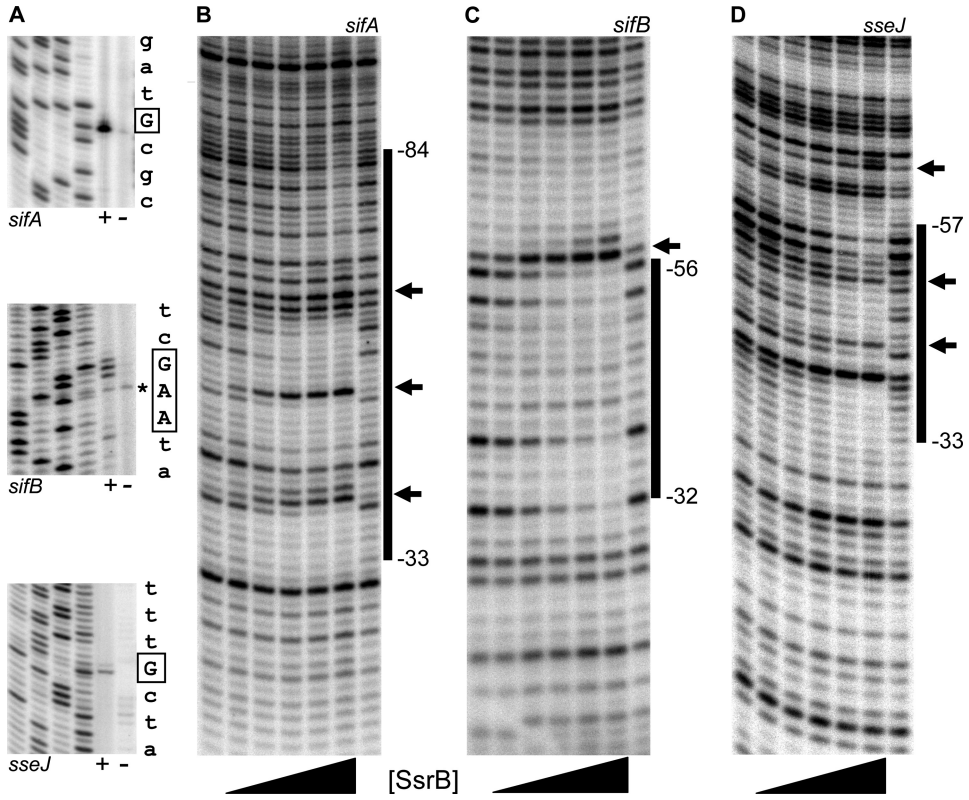

FIGURE 1. **SsrB$_C$ binds upstream of the *sifA*, *sifB*, and *sseJ* promoters.** *A*, promoters were mapped by primer extension on RNA from an *hns* null strain (+) and its *ssrB* null isogenic derivative (−) (14, 23). Gene-specific primers are indicated *below* each gel, and from *left to right* each panel contains C, T, A, and G sequencing ladders. The sequence to the *right* of each panel represents DNA flanking the start sites, which are indicated by *boxed letters*. The *asterisk* indicates a nonspecific primer extension product not observed with an alternate *sifB* primer. The *sifB* +1 coordinate was defined as the G position. *B–D,* DNase I footprinting (*B*) *sifA*, (*C*) *sifB,* and (*D*) *sseJ*. The flanking lanes of each panel contain DNase I-only ladders. Lanes containing SsrB$_C$ (indicated by the *triangle* below each panel) contain, from *left to right*, 25, 100, 200, 400, and 800 nM protein. The *black bars* indicate regions of protection, and predominant hypersensitive sites are represented by *arrows*. Binding coordinates are relative to the transcription start sites identified in *A* and were determined using DNA sequencing ladders as described previously (23).

(compare with pH 8.0) in the wild type background was similarly robust (85-fold; supplemental Fig. 1, *panel B*). Similar results were observed with *sifB* and *sseJ* where the pH induction and *ssrB* dependence was between ~50- and 900-fold (supplemental Fig. 1).

SPI-2 Effector Genes Are Repressed by hns—Previous array studies revealed preferential binding of H-NS to horizontally acquired AT-rich DNA, including the *sifA*, *sifB,* and *sseJ* loci (13, 14). To quantify the repression of *sifA*, *sifB,* and *sseJ* by *hns*, we used qRT-PCR to compare transcript levels in an *hns* mutant under SPI-2-inducing (pH 5.8; Fig. 2, *solid bars*) and noninducing conditions (pH 7.4; Fig. 2, *open bars*). As observed in Fig. 2, acidic pH was a strong inducing signal for *sifA*, *sifB,* and *sseJ* transcription (compare the *red solid* and *open pairs* of *bars* for each gene). In the absence of *hns* (Fig. 2, *black bars*), high expression levels were observed even under noninducing pH (compare the *black solid* and *open pairs of bars* for each gene). Thus, acid pH is not required for transcription in the absence of *hns*. The dependence on *ssrB* for transcription was verified under the different growth conditions required for the *hns* mutant (Fig. 2, see the *blue bars* for each gene).

SsrB$_C$ Stimulates Transcription of sifA, sifB, and sseJ in Vitro in the Absence of Additional Factors—To determine whether SsrB could directly activate transcription, we used

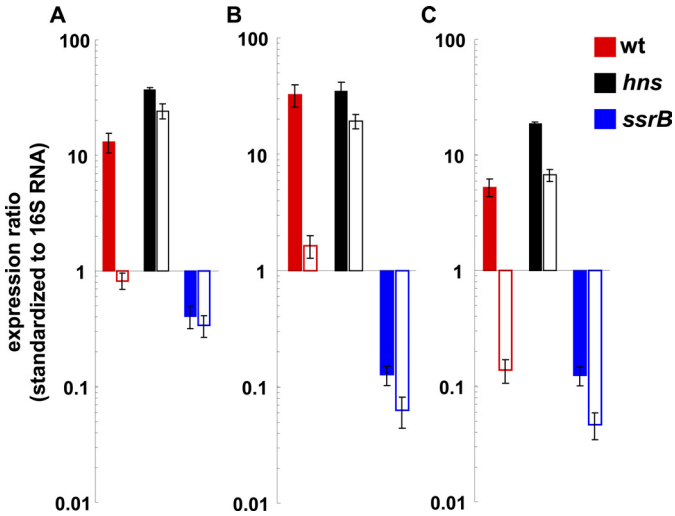

FIGURE 2. **Transcription of *sifA*, *sifB,* and *sseJ* is significantly de-repressed in an *hns* mutant at both inducing (5.8) and noninducing (7.4) pH.** qRT-PCR was used to determine the extent of *hns* silencing of *sifA*, *sifB,* and *sseJ* transcript levels. Reactions were performed with the indicated gene-specific primers and RNA harvested from wild type, *hns*, or *ssrB* null strains grown in PCN minimal medium at inducing (5.8; *solid bars*) or noninducing (7.4; *open bars*) pH. Transcript levels were normalized to 16 S RNA as described under "Experimental Procedures." *Error bars* represent ±1 S.D. The *hns* mutants required PCN minimal medium for growth and are thus not directly comparable with supplemental Fig. 1 where RNA was harvested after growth in N9 minimal medium.

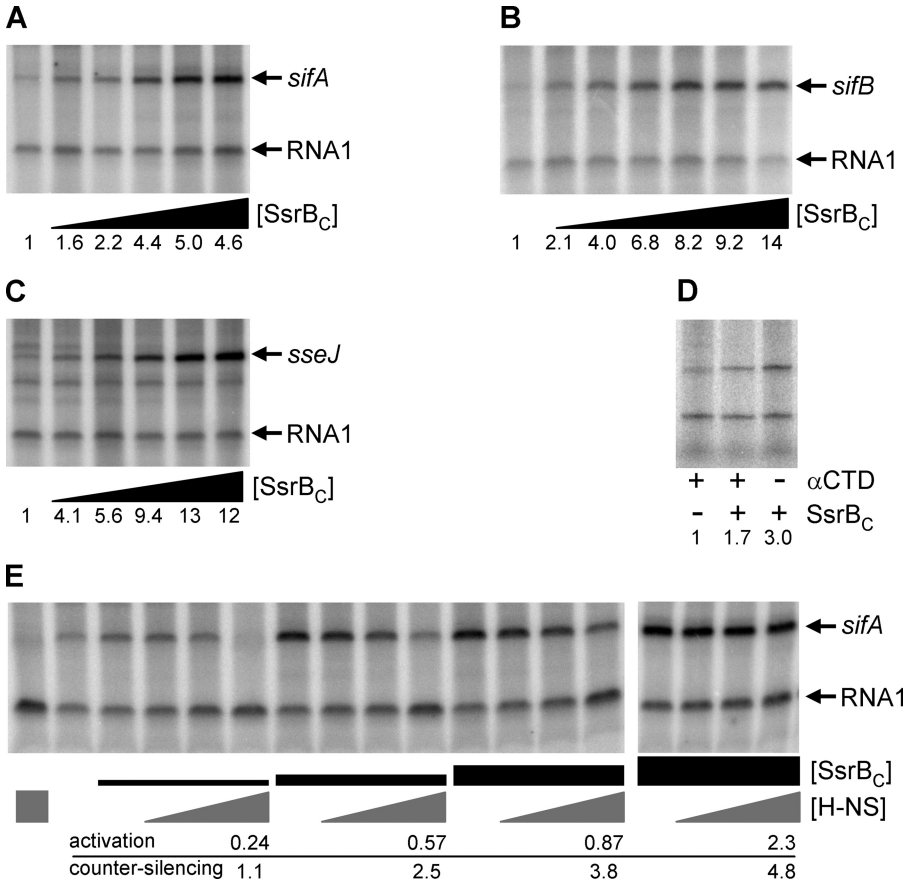

FIGURE 3. **SsrB$_C$ directly activates transcription of *sifA, sifB,* and *sseJ* and overcomes silencing by H-NS.** *A–C* and *E, in vitro* transcription with supercoiled template was used to test the ability of SsrB$_C$ to directly activate transcription of *sifA* (*A*), *sifB* (*B*), and *sseJ* (*C*). The 110-nt RNA-1 internal control transcripts are indicated. Subsequent lanes of each panel contain, from *left to right*, 0, 12.5, 25, 50, 100, and 200 nM SsrB$_C$ for *sifA* and *sseJ*; the concentration range employed for *sifB* is 0, 6.25, 12.5, 25, 50, 100, and 200 nM. The gene-specific transcripts are indicated by *arrows*. *D,* αCTD of RNAP is not required for SsrB$_C$ activation of *sifA*. *In vitro* transcription was performed with 20 nM His$_6$-β′ RNAP or a derivative containing a truncation of αCTD. Each lane contains 20 nM RNAP with (+) or without (−) αCTD. The presence (+) of absence (−) of 50 nM SsrB$_C$ is also indicated. *A–D*, the fold induction (0 nM SsrB$_C$ = 1) is indicated *below*. *E,* SsrB$_C$ was added to *sifA* transcription template pre-bound with H-NS to examine counter-silencing of transcription. The *left-most lane* contains 200 nM H-NS, and the *2nd lane from the left* contains only RNAP. The SsrB$_C$ concentrations employed (indicated by *black boxes*) were 25, 50, 100, and 200 nM. The relative H-NS concentrations (50, 100, or 200 nM) are indicated by *gray triangles*. The activation (0 nM SsrB$_C$ = 1) and counter-silencing (200 nM H-NS = 1) ratios as described in the text are indicated for each reaction containing 200 nM H-NS and the indicated concentration of SsrB$_C$.

purified SsrB$_C$ in an *in vitro* transcription assay. Our initial assays using linear DNA were unsuccessful. Thus, we cloned the *sifA*, *sifB,* and *sseJ* promoter regions into plasmid pRLG770 (30), which contains a strong transcriptional terminator and a small noncoding RNA (RNA-1; 110 nts) that serves as an internal control and molecular weight marker. The results of representative multiple round transcription assays are depicted in Fig. 3. The *left-most lane* of each panel in Fig. 3 contains only RNAP. The subsequent lanes in Fig. 3 contain, from *left to right*, increasing concentrations of SsrB$_C$ as indicated in the figure legend. In Fig. 3*A*, addition of 100 nM SsrB$_C$ results in a 5-fold induction of a 140-nt *sifA* transcript compared with the absence of SsrB$_C$. Further addition of SsrB$_C$ typically results in less induction (*e.g.* ~4.5-fold at 200–300 nM). Similar studies with OmpR did not activate transcription (data not shown). Thus, in contrast to previous reports (40) activation of *sifA* by OmpR is indirect, working through SsrB. Fig. 3*C* depicts reactions containing *sseJ* template; the results reveal a 13-fold increase in *sseJ* transcription in response to 100 nM SsrB$_C$. At 5 nM RNAP, transcription of *sifB* was induced 14-fold upon addition of 200 nM SsrB$_C$ (Fig. 3*B*). At higher concentrations of RNAP, activation was less robust (data not shown). Thus, our results indicate that SsrB$_C$ is able to directly activate transcription in the absence of additional factors, although the level of activation was less than we observed *in vivo* (supplemental Fig. 1). This is not surprising, given the reduced complexity of the *in vitro* assay compared with the *in vivo* environment. SsrB$_C$ requires a supercoiled DNA template. This dependence on a supercoiled template was consistent with a role for SsrB$_C$ in bending DNA (see Figs. 1 and 4) (35).

H-NS and SsrB$_C$ Antagonize sifA Transcription in Vitro—The SPI-2 effector genes were de-repressed in an *hns* mutant (to more than wild type levels at inducing pH and ~12–50-fold at noninducing pH, see Fig. 2). Previous ChIP-on-chip arrays demonstrated a direct effect because of H-NS binding *in vivo* (13, 14). Based on these results, we anticipated that SsrB$_C$ would overcome H-NS repression in our *in vitro* transcription system (Fig. 3*E*). In this experiment, H-NS was allowed to bind to DNA prior to the addition of SsrB$_C$ as described under "Experimental Procedures." Reactions were incubated with 50, 100, or 200 nM H-NS as indicated by the

gray triangles or *box* in Fig. 3*E*. The *1st* and *2nd left-most lanes* in Fig. 3*E* contain 200 or 0 nM H-NS, respectively, in the absence of $SsrB_C$. Subsequently, 25, 50, 100, or 200 nM $SsrB_C$ was added as indicated by the relative sizes of the *black boxes* shown in Fig. 3*E*. Activation (0 nM $SsrB_C$ = 1) and counter-silencing (0 nM $SsrB_C$, 200 nM H-NS = 1) was determined as described under "Experimental Procedures." For clarity, ratios are shown only for reactions containing $SsrB_C$ and 200 nM H-NS. As $SsrB_C$ is increased to 200 nM, counter-silencing of 200 nM H-NS increases to ~5-fold. In contrast, 25 nM $SsrB_C$ is unable to counter-silence H-NS and activation is reduced 4-fold than in the presence of $SsrB_C$ alone. It is noteworthy that RNA-1 transcript levels are not repressed by H-NS (compare the *1st two lanes* of Fig. 3*E*). Indeed, when H-NS is present in the absence of $SsrB_C$, 7.5 nM RNAP is no longer limiting and results in higher RNA-1 levels. Thus, H-NS selectively silences *sifA* transcription (and not RNA-1), but $SsrB_C$ is able to overcome this repression.

$SsrB_C$ Does Not Require αCTD of RNAP to Stimulate sifA Transcription—The $SsrB_C$-binding site partially overlaps the predicted σ^{70} −35 hexamer, consistent with a CRP-type class II mechanism of activation (Ref. 41 and references therein). Class II promoters are either independent of αCTD or require αCTD for maximal activation but are not absolutely dependent on this subunit of RNAP. To determine whether αCTD was required for $SsrB_C$-dependent activation of *sifA* transcription, we employed a preparation of RNAP containing a truncation of this domain in our *in vitro* transcription system (Fig. 3*D*). $SsrB_C$ was able to activate transcription of *sifA* in the presence (1.7-fold) or absence (3-fold) of αCTD. Thus, the αCTD was not required for $SsrB_C$-dependent transcription of *sifA*. This result is consistent with a CRP-type class II mechanism for activation, but it does not rule out a contribution by αCTD for maximal activation *in vivo* or at other SsrB-dependent promoters with different architectures.

Addition of $SsrB_C$ Displaces H-NS When It Is Bound to DNA in the Polymerized Form and Not the Bridged Form—In a previous study, we discovered that H-NS has two modes of interacting with DNA and that Mg^{2+} or other divalent cations can switch its binding mode without H-NS being released from DNA (26). In the absence of Mg^{2+}, H-NS binding causes the DNA to become stiffer and more elongated (26, 27). At high Mg^{2+} (5 mM or above), H-NS binding leads to DNA folding (bridging), and no apparent stiffening is observed (26, 28). At intermediate Mg^{2+}, both forms of H-NS binding are observed. The mechanism of stiffening binding was also discovered to be the result of H-NS polymerization along the DNA commencing from scattered nucleation sites (26). It was therefore of interest to determine whether one mode of binding was more susceptible to de-repression by $SsrB_C$ (Fig. 4). Our magnetic tweezers setup was described previously (26), in which one end of DNA is tethered to a coverslip and coupled to a magnetic bead at the other end. The extension of naked DNA in response to applied force is shown in the *black squares* (Fig. 4, *A–F*). Addition of H-NS in buffer lacking Mg^{2+} leads to stiffening (26). This is evident as the DNA becomes more extended as the applied force is decreased when compared with naked DNA (Fig. 4*A*, compare *black squares*

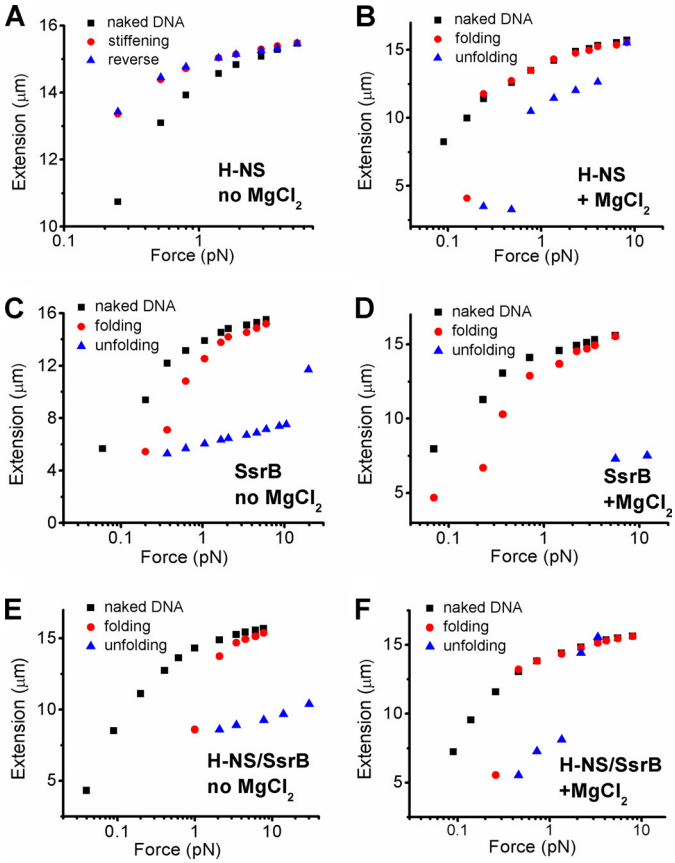

FIGURE 4. **$SsrB_C$ displaces H-NS from DNA-only when bound in polymerization mode.** *A,* H-NS stiffens DNA in the absence of $MgCl_2$. *Black squares* are the extension of DNA in the buffer alone. *Red circles* are the extension of the same DNA in the presence of 600 nM H-NS when the force was gradually reduced. The *blue triangles* are extension of the same DNA when the force was increased. The *red circles* overlapped with the *blue triangles*, indicating that the extension reached equilibrium. The symbols and colors are identical in subsequent panels. *B,* H-NS folds DNA at 10 mM $MgCl_2$. When the force was reduced to <0.3 pN, folding occurred over a large distance within the recording time (*red circles*). The folded DNA could be unfolded at forces >0.8 pN (*blue triangles*). *C,* $SsrB_C$ folds DNA in stiffening buffer (*i.e.* in the absence of $MgCl_2$). The DNA shortens, even at low pN forces. Large scale folding within the recording time window occurred as the force was decreased below 1 pN (*red circles*). In addition, the folded DNA could not be unfolded as the force was reapplied to high tensions (>10 pN; *blue triangles*). *D,* $SsrB_C$ folds DNA in the bridging buffer of H-NS (*i.e.* in 10 mM $MgCl_2$). SsrBc folds DNA in H-NS stiffening buffer, and it can also fold DNA in H-NS bridging buffer (*red circles*). Unlike what we observed with H-NS (*B*), the SsrB-folded DNA cannot be unfolded under large tensions (*blue squares*). *E,* $SsrB_C$ folds DNA in the presence of H-NS bound in the stiffening mode (no $MgCl_2$). In the presence of 600 nM H-NS (bound to DNA in stiffening mode), addition of 300 nM $SsrB_C$ leads to DNA folding (*red circles*). Once the DNA is folded by $SsrB_C$, it cannot be unfolded even under large tensions (*blue triangles*). *F,* DNA folding in the presence of 600 nM H-NS, 300 nM $SsrB_C$, in bridging buffer (pH 7.4, 50 mM KCl, 10 mM $MgCl_2$, 24 °C). At high $MgCl_2$, DNA is folded (*red circles*) and unfolded (*blue triangles*) at forces observed with H-NS alone. Thus, when H-NS is bound to DNA in the bridging mode, it appears to be inert to addition of $SsrB_C$.

with *red circles* at each force measurement). When the force is then increased (Fig. 4*A*, *blue triangles*), the DNA extension overlaps during the force decreasing process (*i.e. blue triangles* and *red circles overlap*), indicating that the binding reaches a steady state within the experimental time scale. At high Mg^{2+}, H-NS causes significant folding (*i.e.* bridging) of DNA when the force is reduced to below 0.2 pN (Fig. 4*B*, *red circles*). When the force is increased (Fig. 4*B*, *blue triangles*), the DNA becomes extended again. However, the resulting

extension is less than naked DNA within the recording time until the force reaches 10 pN. In the region of hysteresis (*i.e.* the nonoverlapping region), a steady state is not reached. In contrast, addition of $SsrB_C$ at either no (Fig. 4*C*) or high ((Fig. 4*D*) Mg^{2+} leads to DNA folding, *i.e.* there is a dramatic shortening of the DNA. This folded DNA cannot be unfolded, even when held at forces >10 pN for extended times. Thus, H-NS and SsrB proteins have distinct and distinguishable effects on DNA as a consequence of binding.

We next examined the effect of $SsrB_C$ addition after H-NS was bound to DNA in the stiffening mode (Fig. 4*E*). As the force was gradually decreased, DNA extension decreased dramatically, *i.e.* the DNA was folded (Fig. 4*E*, *red circles*). Because folding never occurs with just H-NS bound to DNA in buffer lacking Mg^{2+} (Fig. 4*A*), this result must mean that $SsrB_C$ displaces H-NS from the DNA. Consequently, $SsrB_C$ binding then induces folding, as observed with $SsrB_C$ alone (Fig. 4*C*). Reapplication of the force did not lead to unfolding of the DNA (Fig. 4*E, blue triangles*), as also observed with $SsrB_C$ alone (Fig. 4*C*). In other words, the $SsrB_C$ binding mode (*i.e.* DNA folding) predominates under conditions where H-NS would promote polymerization (*i.e.* DNA stiffening). The experiment with both proteins was repeated in buffer containing high Mg^{2+} (Fig. 4*F*). Not unexpectedly, decreasing the force caused folding of the DNA, as seen with either protein alone (Fig. 4, *B* and *D*). Intriguingly, reapplication of force resulted in unfolding of the DNA (Fig. 4*F, blue triangles*), as seen with H-NS alone (Fig. 4*B*) and despite the presence of SsrB. Thus, $SsrB_C$ displaces H-NS from DNA only when it is bound in the polymerization or stiffening mode. At high Mg^{2+}, when H-NS is bound in bridging mode, $SsrB_C$ does not displace it. It is noteworthy that 1 mM Mg^{2+}, which is present in the stiffening buffer DNA (26), is the physiologically relevant concentration to which *Salmonella* is exposed when in the SCV (42).

DISCUSSION

SsrB Employs Two Mechanisms to Regulate Transcription, Direct Activation and Relief of H-NS Silencing—The architectures of the *sifA*, *sifB,* and *sseJ* promoters were defined using a combination of primer extension and DNase I protection footprinting assays. Our results revealed that SsrB directly regulates transcription at these promoters by binding upstream from, and perhaps overlapping, their respective −35 hexamers (Fig. 1). We then employed *in vitro* transcription to determine whether SsrB bound at these sites was sufficient for recruitment of RNAP and activation of transcription (Fig. 3); indeed, the combination of both SsrB and RNAP was necessary and sufficient to activate transcription using supercoiled DNA templates. The αCTD of RNAP was dispensable for activation, which suggests a CRP-type class II activation mechanism (41) and is in agreement with our finding that SsrB binding sites likely overlap the putative −35 hexamers of each promoter. Thus, one mode of action employed by SsrB to regulate transcription is direct activation.

H-NS is a nucleoid structuring protein and a global regulator of transcription in *Salmonella* and related Gram-negative bacteria such as *E. coli* and *Yersinia* (43–45). Our previous work and results from other groups determined that *hns* had a major effect on silencing transcription of SPI-2 and SPI-2 co-regulated genes (13, 14, 23). We quantified the extent of *hns* repression of SPI-2 co-regulated genes using qRT-PCR. In the absence of *hns*, a significant de-repression of *sifA*, *sifB,* and *sseJ* transcription under noninducing conditions, pH 7.4, was observed. Thus, *hns* strongly silences effector gene transcription (Fig. 2), as we also observed for genes within the SPI-2 cluster. The ability of SsrB to counter H-NS silencing was further demonstrated using *in vitro* transcription assays (Fig. 3). H-NS specifically repressed transcription of *sifA*, but this repression was antagonized by the presence of SsrB. Furthermore, DNase I footprinting suggests that SsrB directly competes for binding with H-NS at *sifA* (supplemental Fig. 2). Experiments with magnetic tweezers also indicated that SsrB binding to DNA led to DNA folding while displacing H-NS (Fig. 4). This dual mechanism is shared by RovA, a SlyA homologue from *Yersinia*, which both relieves H-NS silencing and directly activates virulence gene expression (46). In contrast, the response regulator PhoP cannot directly activate gene expression in the presence of H-NS unless SlyA is also present to counteract silencing (47).

$SsrB_C$ Displaces H-NS from DNA Only When Bound in the Polymerization Mode—H-NS can switch between polymerization (*i.e.* nucleation) and bridging DNA binding conformations in response to divalent cations (*e.g.* Mg^{2+}), and we showed that it is the polymerization mode that prevails under physiological conditions (26). Here, we examined which of these two DNA binding conformations of H-NS is sensitive to de-repression by SsrB. Single molecule experiments using magnetic tweezers revealed that SsrB was able to promote DNA folding under conditions that normally direct H-NS polymerization on DNA (Fig. 4*E*) (26). In contrast, 10 mM Mg^{2+} promoted H-NS bridging of DNA, and this DNA binding conformation was insensitive to the presence of SsrB (Fig. 4*F*). Folding by H-NS occurred at a much lower force (~0.2 pN *versus* several pN), and the DNA could be unfolded at ~1 pN or above (Fig. 4*B*). In contrast, when only SsrB was present in 10 mM Mg^{2+} bridging buffer (Fig. 4*C*) or with H-NS in stiffening buffer lacking Mg^{2+} (Fig. 4*E*), the DNA could not be unfolded, even under forces of >10 pN. Our previous results suggested that H-NS bound to DNA in the stiffening mode was the relevant mode and are further supported by our findings here. This is the form in which silencing can be countered by SsrB. Our results are consistent with a previously reported value of ~1 mM for intracellular Mg^{2+} concentration (42) in which the polymerized form would prevail.

Acknowledgments—We are grateful to Wilma Ross and Rick Gourse (University of Wisconsin) for invaluable assistance with in vitro transcription assays, William Navarre (University of Toronto) for helpful discussions, and Stephen J. Libby (University of Washington) for valuable comments on the manuscript.

REFERENCES

1. Stein, M. A., Leung, K. Y., Zwick, M., Garcia-del Portillo, F., and Finlay, B. B. (1996) *Mol. Microbiol.* **20,** 151–164
2. Brumell, J. H., Goosney, D. L., and Finlay, B. B. (2002) *Traffic* **3,**

407–415
3. Boucrot, E., Henry, T., Borg, J. P., Gorvel, J. P., and Méresse, S. (2005) *Science* **308,** 1174–1178
4. Salcedo, S. P., and Holden, D. W. (2003) *EMBO J.* **22,** 5003–5014
5. Garcia-del Portillo, F., Zwick, M. B., Leung, K. Y., and Finlay, B. B. (1993) *Proc. Natl. Acad. Sci. U.S.A.* **90,** 10544–10548
6. Ohlson, M. B., Huang, Z., Alto, N. M., Blanc, M. P., Dixon, J. E., Chai, J., and Miller, S. I. (2008) *Cell Host Microbe* **4,** 434–446
7. Beuzón, C. R., Méresse, S., Unsworth, K. E., Ruíz-Albert, J., Garvis, S., Waterman, S. R., Ryder, T. A., Boucrot, E., and Holden, D. W. (2000) *EMBO J.* **19,** 3235–3249
8. Jackson, L. K., Nawabi, P., Hentea, C., Roark, E. A., and Haldar, K. (2008) *Proc. Natl. Acad. Sci. U.S.A.* **105,** 14141–14146
9. Ohlson, M. B., Fluhr, K., Birmingham, C. L., Brumell, J. H., and Miller, S. I. (2005) *Infect. Immun.* **73,** 6249–6259
10. Nawabi, P., Catron, D. M., and Haldar, K. (2008) *Mol. Microbiol.* **68,** 173–185
11. Ruiz-Albert, J., Yu, X. J., Beuzón, C. R., Blakey, A. N., Galyov, E. E., and Holden, D. W. (2002) *Mol. Microbiol.* **44,** 645–661
12. Freeman, J. A., Ohl, M. E., and Miller, S. I. (2003) *Infect. Immun.* **71,** 418–427
13. Lucchini, S., Rowley, G., Goldberg, M. D., Hurd, D., Harrison, M., and Hinton, J. C. (2006) *PLoS Pathog.* **2,** e81
14. Navarre, W. W., Porwollik, S., Wang, Y., McClelland, M., Rosen, H., Libby, S. J., and Fang, F. C. (2006) *Science* **313,** 236–238
15. Feng, X., Walthers, D., Oropeza, R., and Kenney, L. J. (2004) *Mol. Microbiol.* **54,** 823–835
16. Feng, X., Oropeza, R., and Kenney, L. J. (2003) *Mol. Microbiol.* **48,** 1131–1143
17. Lee, A. K., Detweiler, C. S., and Falkow, S. (2000) *J. Bacteriol.* **182,** 771–781
18. Kelly, A., Goldberg, M. D., Carroll, R. K., Danino, V., Hinton, J. C., and Dorman, C. J. (2004) *Microbiology* **150,** 2037–2053
19. Miller, S. I., Kukral, A. M., and Mekalanos, J. J. (1989) *Proc. Natl. Acad. Sci. U.S.A.* **86,** 5054–5058
20. Miao, E. A., Freeman, J. A., and Miller, S. I. (2002) *J. Bacteriol.* **184,** 1493–1497
21. Bijlsma, J. J., and Groisman, E. A. (2005) *Mol. Microbiol.* **57,** 85–96
22. Kato, A., and Groisman, E. A. (2008) *Adv. Exp. Med. Biol.* **631,** 7–21
23. Walthers, D., Carroll, R. K., Navarre, W. W., Libby, S. J., Fang, F. C., and Kenney, L. J. (2007) *Mol. Microbiol.* **65,** 477–493
24. Worley, M. J., Ching, K. H., and Heffron, F. (2000) *Mol. Microbiol.* **36,** 749–761
25. Fang, F. C., and Rimsky, S. (2008) *Curr. Opin. Microbiol.* **11,** 113–120
26. Liu, Y., Chen, H., Kenney, L. J., and Yan, J. (2010) *Genes Dev.* **24,** 339–344
27. Amit, R., Oppenheim, A. B., and Stavans, J. (2003) *Biophys. J.* **84,** 2467–2473
28. Dame, R. T., Noom, M. C., and Wuite, G. J. (2006) *Nature* **444,** 387–390
29. Mayer, M. P. (1995) *Gene* **163,** 41–46
30. Ross, W., Thompson, J. F., Newlands, J. T., and Gourse, R. L. (1990) *EMBO J.* **9,** 3733–3742
31. Ross, W., and Gourse, R. L. (2009) *Methods* **47,** 13–24
32. Yan, J., Skoko, D., and Marko, J. F. (2004) *Phys. Rev. E Stat. Nonlin. Soft Matter Phys.* **70,** 011905
33. Miao, E. A., and Miller, S. I. (2000) *Proc. Natl. Acad. Sci. U.S.A.* **97,** 7539–7544
34. Maris, A. E., Sawaya, M. R., Kaczor-Grzeskowiak, M., Jarvis, M. R., Bearson, S. M., Kopka, M. L., Schröder, I., Gunsalus, R. P., and Dickerson, R. E. (2002) *Nat. Struct. Biol.* **9,** 771–778
35. Carroll, R. K., Liao, X., Morgan, L. K., Cicirelli, E. M., Li, Y., Sheng, W., Feng, X., and Kenney, L. J. (2009) *J. Biol. Chem.* **284,** 12008–12019
36. Beuzón, C. R., Banks, G., Deiwick, J., Hensel, M., and Holden, D. W. (1999) *Mol. Microbiol.* **33,** 806–816
37. Hansen-Wester, I., Stecher, B., and Hensel, M. (2002) *Infect. Immun.* **70,** 1403–1409
38. Nikolaus, T., Deiwick, J., Rappl, C., Freeman, J. A., Schröder, W., Miller, S. I., and Hensel, M. (2001) *J. Bacteriol.* **183,** 6036–6045
39. Rappl, C., Deiwick, J., and Hensel, M. (2003) *FEMS Microbiol. Lett.* **226,** 363–372
40. Mills, S. D., Ruschkowski, S. R., Stein, M. A., and Finlay, B. B. (1998) *Infect. Immun.* **66,** 1806–1811
41. Savery, N., Rhodius, V., and Busby, S. (1996) *Philos. Trans. R. Soc. Lond. B. Biol. Sci.* **351,** 543–550
42. Martin-Orozco, N., Touret, N., Zaharik, M. L., Park, E., Kopelman, R., Miller, S., Finlay, B. B., Gros, P., and Grinstein, S. (2006) *Mol. Biol. Cell* **17,** 498–510
43. Baños, R. C., Pons, J. I., Madrid, C., and Juárez, A. (2008) *Microbiology* **154,** 1281–1289
44. Oshima, T., Ishikawa, S., Kurokawa, K., Aiba, H., and Ogasawara, N. (2006) *DNA Res.* **13,** 141–153
45. Cathelyn, J. S., Ellison, D. W., Hinchliffe, S. J., Wren, B. W., and Miller, V. L. (2007) *Mol. Microbiol.* **66,** 189–205
46. Tran, H. J., Heroven, A. K., Winkler, L., Spreter, T., Beatrix, B., and Dersch, P. (2005) *J. Biol. Chem.* **280,** 42423–42432
47. Perez, J. C., Latifi, T., and Groisman, E. A. (2008) *J. Biol. Chem.* **283,** 10773–10783